Circulation
Heart Failure
JOURNAL OF THE AMERICAN HEART ASSOCIATION

Septal Deformation Patterns Delineate Mechanical Dyssynchrony and Regional Differences in Contractility : Analysis of Patient Data Using a Computer Model

Geert E. Leenders, Joost Lumens, Maarten J. Cramer, Bart W.L. De Boeck, Pieter A. Doevendans, Tammo Delhaas and Frits W. Prinzen

Circ Heart Fail 2012;5;87-96; originally published online October 6, 2011;
DOI: 10.1161/CIRCHEARTFAILURE.111.962704
Circulation: Heart Failure is published by the American Heart Association. 7272 Greenville Avenue, Dallas, TX 72514
 Print ISSN: 1941-3289. Online ISSN: 1941-3297

Septal Deformation Patterns Delineate Mechanical Dyssynchrony and Regional Differences in Contractility

Analysis of Patient Data Using a Computer Model

Geert E. Leenders, MD*; Joost Lumens, PhD*; Maarten J. Cramer, MD, PhD; Bart W.L. De Boeck, MD, PhD; Pieter A. Doevendans, MD, PhD; Tammo Delhaas, MD, PhD; Frits W. Prinzen, PhD

Background—Response to cardiac resynchronization therapy depends both on dyssynchrony and (regional) contractility. We hypothesized that septal deformation can be used to infer integrated information on dyssynchrony and regional contractility, and thereby predict cardiac resynchronization therapy response.

Methods and Results—In 132 cardiac resynchronization therapy candidates with left bundle branch block (LBBB)-like electrocardiogram morphology (left ventricular ejection fraction 19±6%; QRS width 170±23 ms), longitudinal septal strain was assessed by speckle tracking echocardiography. To investigate the effects of dyssynchronous activation and differences in septal and left ventricular free wall contractility on septal deformation pattern, we used the CircAdapt computer model of the human heart and circulation. In the patients, 3 characteristic septal deformation patterns were identified: LBBB-1=double-peaked systolic shortening (n=28); LBBB-2=early systolic shortening followed by prominent systolic stretching (n=34); and LBBB-3=pseudonormal shortening with less pronounced late systolic stretch (n=70). LBBB-3 revealed more scar (2 [2–5] segments) compared with LBBB-1 and LBBB-2 (both 0 [0–1], $P<0.05$). In the model, imposing a time difference of activation between septum and left ventricular free wall resulted in pattern LBBB-1. This transformed into pattern LBBB-2 by additionally simulating septal hypocontractility, and into pattern LBBB-3 by imposing additional left ventricular free wall or global left ventricular hypocontractility. Improvement of left ventricular ejection fraction and reduction of left ventricular volumes after cardiac resynchronization therapy were most pronounced in LBBB-1 and worst in LBBB-3 patients.

Conclusions—A double-peaked systolic septal deformation pattern is characteristic for LBBB and results from intraventricular dyssynchrony. Abnormal contractility modifies this pattern. A computer model can be helpful in understanding septal deformation and predicting cardiac resynchronization therapy response. **(*Circ Heart Fail*. 2012; 5:87-96.)**

Key Words: bundle-branch block ■ cardiac resynchronization therapy ■ dyssynchrony ■ echocardiography ■ myocardial contraction

Left bundle branch block (LBBB) causes a disparity of electrical activation of the heart that results in a prominent electrical and mechanical activation delay (dyssynchrony) between the right and the left ventricle (LV), and between the septum and the left ventricle free wall (LVFW).[1–3] Such activation delays give way to reciprocal contractile interactions that present as back and forth shortening and stretching of the myocardium (mechanical discoordination), thereby instigating inefficient myocardial contraction and relaxation and ultimately leading to heart failure and myocardial remodeling.[3]

Clinical Perspective on p 96

Because the interventricular septum is centered amid the discoordinated right ventricular (RV) and LV walls, and is additionally subject to altered loading by the abnormal right-to-left transseptal pressure gradient, it is particularly susceptible to motion and deformation abnormalities caused

Received April 17, 2011; accepted October 3, 2011.

From the Department of Cardiology, University Medical Center Utrecht (G.E.L., M.J.C., P.A.D.), Utrecht, the Netherlands; Departments of Physiology and Biomedical Engineering, Cardiovascular Research Institute Maastricht (J.L., T.D., F.W.P.), Maastricht, the Netherlands; Kantonsspital Luzern (B.W.L.D.B.), Luzern, Switzerland.

*Drs Leenders and Lumens contributed equally to this work.

The online-only Data Supplement is available with this article at http://circheartfailure.ahajournals.org/lookup/suppl/doi:10.1161/CIRCHEARTFAILURE. 111.962704/-/DC1.

Correspondence to Geert E. Leenders, MD, Department of Cardiology, University Medical Center Utrecht, P.O. Box 855500, 3508 GA Utrecht, the Netherlands. E-mail g.e.h.leenders@umcutrecht.nl

Circ Heart Fail **is available at http://circheartfailure.ahajournals.org** **DOI: 10.1161/CIRCHEARTFAILURE.111.962704**

by LBBB.[4,5] Abnormalities of septal motion and deformation have therefore repeatedly been used to identify the mechanical consequences of LBBB.[6–8] In line with the latter, parameters of mechanical dyssynchrony often rely on abnormal (early) septal motion or deformation for the identification of mechanical dyssynchrony and the prediction of response to cardiac resynchronization therapy (CRT).[9]

Besides disparity in timing of mechanical activation and the abnormal transseptal pressure gradient, which are both primarily influenced by the dispersed electrical activation, regional heterogeneity in myocardial tissue properties (eg, contractility and scarring) may additionally influence myocardial deformation.[6,10–13] Local tissue properties of the septum and LVFW may thereby either mask or mimic septal deformation abnormalities caused by mechanical dyssynchrony.

We hypothesized that the septal deformation pattern can be used to infer integrated information on dyssynchrony and regional contractility and thereby predict CRT response. In order to assess this hypothesis, we evaluated a patient population, with LBBB and systolic heart failure, by echocardiographic deformation imaging and additionally used the multiscale CircAdapt model of the human heart and circulation[14,15] to further elucidate the influence of each factor individually on septal deformation.

Methods

Study Population and Protocol

The study population constituted a consecutive cohort of patients (enrolled in the University Medical Center Utrecht between August 2005 and April 2009) undergoing CRT because of severe medication refractory heart failure (New York Heart Association [NYHA] class III–IV, left ventricle ejection fraction [LVEF] <35%) and evidence of conduction disturbances (QRS ≥120 ms) with an LBBB-like morphology on the surface electrocardiogram. Eight patients with poor echocardiographic window, and 1 patient undergoing coronary artery and mitral valve surgery within 6 months before CRT, were excluded from the analysis. Echocardiographic and clinical characteristics were prospectively assessed in all patients before and 6 months after CRT. The execution of the study complied to the principles outlined in the Declaration of Helsinki on research in human subjects and to the procedures of the local Medical Ethics Committee.

Echocardiographic Protocol

Our echocardiographic protocol has been described in detail elsewhere.[6] In brief, all data were obtained on a Vivid 7 ultrasound machine (General Electric, Milwaukee, MN) using a broadband M3S transducer for Doppler and 2-dimensional imaging. A minimum of 3 loops were acquired at breath hold and analyzed offline (Echopac version 6.0.1, General Electric). LVEF, left ventricle end-systolic, and end-diastolic volumes indexed for body surface area ($LVESV_i$ and $LVEDV_i$, respectively) were measured by biplane Simpson method. Mitral regurgitation effective regurgitant orifice (MRERO) was quantified by the proximal isovelocity surface area method. Interventricular septal and left ventricle posterior wall thickness were measured on M-Mode in the parasternal long axis view. LV end-diastolic sphericity was calculated by the ratio of the minor axis to the major axis length of the LV, as derived from the apical 4-chamber view.

The LV was divided into 16 segments according to the recommendations of the American Society of Echocardiography.[16] Segments which displayed akinesis or dyskinesis in combination with a disproportionate local wall thinning and hyperreflectivity in comparison with adjacent contractile segments were scored as "scarred."[17]

For offline deformation imaging, additional single wall images of the septum and lateral wall were prospectively acquired from the standard apical views at 51 to 109 frames per second. Timing of mitral and aortic valve opening and closure, as derived from Doppler flow patterns over the left-sided valves, served as cardiac event timing markers.

Deformation Analysis

Speckle tracking software was used to derive septal and lateral LVFW deformation from the single wall recordings. Deformation was measured from base to apex, covering the entire wall thickness (Figure 1). Global longitudinal deformation (ie, calculated over the entire length of the wall) was temporally aligned using onset of the QRS complex as zero reference. Septal deformation patterns were classified based on the sequence of septal shortening and stretching during LV systole (ie, between mitral and aortic valve closure). Peak systolic strain was defined where systolic shortening converted into stretching, and the absolute strain value was maximally negative. More than 1 systolic peak was adjudicated only if the amplitudes of the peaks were within 150% relative range of each other; in all other cases, the dominant peak was considered the only systolic peak (Figure 1).

Device Implantation

Right atrial, RV, and LV leads were placed conventionally and connected to a CRT device as described previously.[6] Atrioventricular and ventriculoventricular intervals were optimized either by maximizing the invasively determined maximum rate of LV pressure rise (n=92) or by intracardiac electrogram-based device algorithms (n=40).

CircAdapt Model

The effects of dyssynchronous activation and regional LV contractility differences on septal deformation were investigated using the multiscale CircAdapt model of the cardiovascular system.[14,15] The model contains modules representing myocardial walls, cardiac valves, large blood vessels, and peripheral resistances. It can simulate realistic beat-to-beat cardiovascular mechanics and hemodynamics under a wide variety of (patho-) physiological circumstances.[15,18–20] To incorporate mechanical ventricular interaction, 3 thick-walled segments representing the LVFW, the interventricular septum, and the RV free wall are mechanically coupled.[15] From the geometry of each wall, representative local myofiber strain is calculated. From myofiber strain, myofiber stress is determined using a 3-element muscle model describing active and passive cardiac myofiber mechanics.[15] The latter model incorporates known sarcomere properties, such as velocity of sarcomere shortening as function of passive stretch, and strength and duration of activation as function of sarcomere length.[21–23] Global left and right ventricular pump mechanics are related to representative myofiber mechanics in the 3 ventricular walls, using the principle of conservation of energy. Because the pericardium can significantly modulate ventricular interaction,[24–27] the effect of the pericardium on ventricular mechanics was included in the model (see the online-only supplement).

Simulation of Normal Cardiovascular Mechanics and Hemodynamics

First, the CircAdapt model was used to obtain the NORMAL simulation, representing the cardiovascular system under baseline resting conditions. Onset of mechanical activation of the 3 ventricular walls was synchronous, with underlying identical electromechanical delays in all walls. Myocardial contractility was normal. Size and mass of cardiac walls and large blood vessels were tuned to obtain normal cardiac output (5.1 l/min), mean arterial blood pressure (92 mm Hg), and heart rate (70 bpm) at tissue-specific physiological levels of mechanical load.[14,15] Changes in local deformation in subsequent simulations represent the effect of abnormal electrical activation, reduction of contractility, and acute adjustments

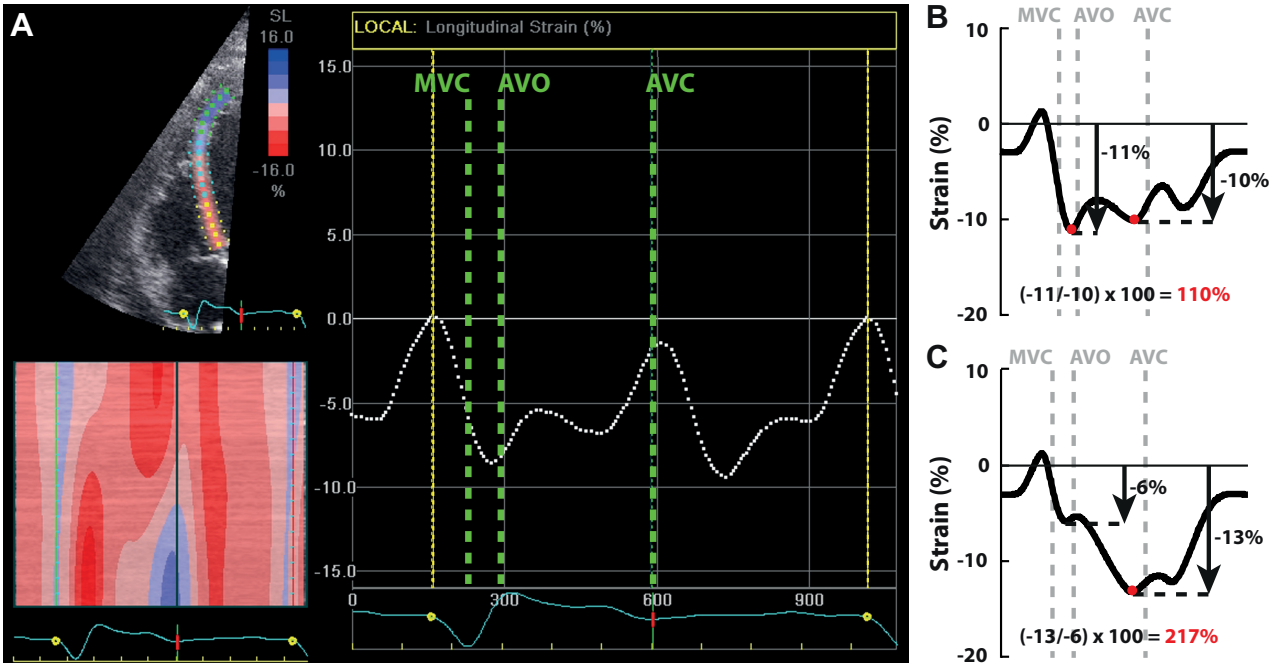

Figure 1. Measurement of septal deformation and adjudication of peaks. Longitudinal septal deformation is derived from single wall images (panel **A**, upper left corner). The dotted white line in panel **A** represents global deformation (negative slopes indicate shortening) of the interventricular septum and is used for septal deformation pattern classification. Aortic valve opening (AVO) and closure (AVC) define the ejection period. Onset of the QRS complex (yellow circles and vertical lines) is used as zero strain reference. Adjudicated peaks are identified within the systolic period (ie, between mitral valve closure [MVC] and aortic valve opening) and are indicated by red dots in panels **B** and **C**. Panel **B** shows a pattern where the amplitude of the first peak is within 150% of the second peak, and 2 systolic peaks are adjudicated. Panel **C** shows an example where the amplitude of the second peak is >150% that of the first peak, leading to the definition of a "late peak."

required to maintain normal levels of cardiac output and blood pressure.

Simulation of Ventricular Mechanical Dyssynchrony and Hypocontractility

To assess the effect of dyssynchronous mechanical activation on septal deformation, onset of septal and LVFW mechanical activation were delayed with respect to that of the RV free wall by 25 and 50 ms for the septum and 25, 50, 75, and 100 ms for the LVFW. In each simulation, septal deformation was quantified as the percentage change in sarcomere length, with respect to reference sarcomere length at onset of RV free wall mechanical activation (ie, the first ventricular activation), which was similar in all simulations (≈30 ms after right atrial activation) and was assumed to correspond best to the zero-strain reference in the patients.

To assess the effect of local differences in contractile myofiber function on septal deformation, we reduced myofiber contractility by decreasing isometric active myofiber stress by 30 and 60% in the septum and in the LVFW. These assessments were performed in the simulation with 25 and 75 ms delayed onset of (mean) septal and LVFW activation, respectively. These values were chosen in order to cover the mean timing differences in RV, septum, and LVFW, as observed in human LBBB patients.[1,2] Additionally, to assess the isolated effect of regional contractility changes on septal deformation, hypocontractility simulations were also applied to the NORMAL simulation (online-only supplement).

Statistical Analysis

Statistical analysis was performed using the SPSS statistical software package (SPSS Inc, Chicago, IL). Values are presented as mean and standard deviation or median and interquartile range for continuous variables as appropriate, and as numbers and percentages for categorical variables. Assumptions on homogeneity of variances and normally distributed residuals were checked by Levene test and Q-Q plots, respectively. Comparison of continuous data between subgroups was performed by 1-way analysis of variance. Categorical data was compared by χ^2 or Fischer Exact test. Bonferroni post hoc correction for multiple comparisons was applied when applicable. A probability value <0.05 was considered statistically significant for all analyses.

Results

Study Population

The final study population constituted 132 patients: 93 male (70%), age 65±10 years, LVEF 19±6%, and 19 NYHA IV (14%). The cause of heart failure was ischemic in 69 patients (52%). In total, 27 patients (20%) were previously known with atrial fibrillation. All patients were on stable, maximally tolerated heart failure medication, with angiotensin converting enzyme inhibitors or angiotensin receptor blockers in 117 (89%), β-blockers in 103 (78%), and diuretics in 126 (95%).

In the total population, 3 characteristic patterns of septal deformation could be discerned (Figure 2): LBBB-1=double-peaked systolic shortening in 28 patients (21%); LBBB-2=early pre-ejection shortening peak followed by prominent systolic stretching in 34 patients (26%); and LBBB-3=pseudonormal shortening, with a late-systolic shortening peak followed by less pronounced end-systolic stretch, in 70 patients (53%).

Baseline Characteristics of the Deformation Pattern Subgroups

Table 1 shows the baseline characteristics of the population. In general, patients with LBBB-1 had electrical dyssynchrony

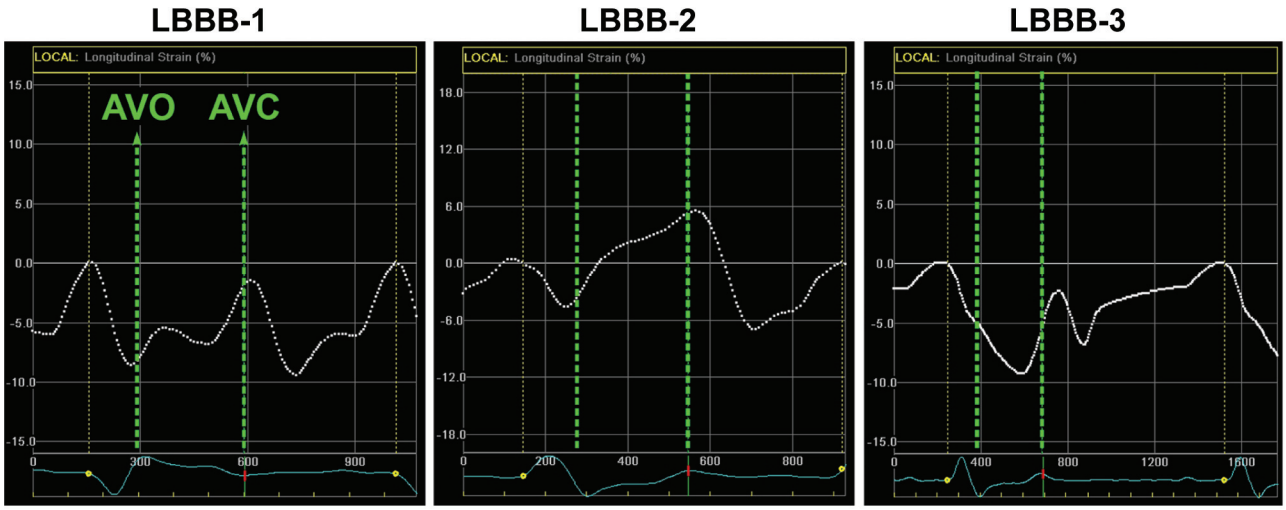

Figure 2. Typical septal deformation patterns. Typical examples of septal deformation patterns in 3 left bundle branch block (LBBB) patients; LBBB-1: double-peaked systolic shortening; LBBB-2: early pre-ejection shortening peak followed by prominent systolic stretch; and LBBB-3: pseudonormal shortening with a late-systolic shortening peak and less pronounced end-systolic stretch. Green vertical lines indicate aortic valve opening (AVO) and closure (AVC).

(evidenced by the broad QRS width) but relatively mild adverse remodeling, as expressed by the moderate dilatation ($LVEDV_i$ and $LVESV_i$), relatively preserved wall thickness (intraventricular septal and left ventricle posterior wall thickness), and only mild mitral regurgitation. LBBB-2 patients had similar electrical dyssynchrony, but were characterized by more pronounced structural adaptation and more globular LV dilatation (as expressed by LV volumes and sphericity),

Table 1. Baseline Characteristics of Septal Deformation Pattern Subgroups

	Septal Deformation Pattern			*P* Value			
Parameter	LBBB-1 (n=28)	LBBB-2 (n=34)	LBBB-3 (n=70)	ANOVA/χ^2	LBBB-1 vs LBBB-2	LBBB-1 vs LBBB-3	LBBB-2 vs LBBB-3
Age (y)	62±12	65±11	67±8	0.150	. . .	. . .	. . .
QRS width (ms)	178±20	176±20	164±23	0.003	1.000	0.012	0.020
Ischemic etiol. (%)	35.7	41.2	64.3	0.012	1.000	0.039	0.105
Scarred segm. (nr)*	0 (0–1)	0 (0–1)	2 (2–5)	<0.001	1.000	0.003	0.003
Sept wall scar (nr)*	0 (0–0)	0 (0–0)	0 (0–2)	0.007	1.000	0.048	0.023
Free wall scar (nr)*	0 (0–1)	0 (0–1)	1 (0–3)	0.002	1.000	0.010	0.013
Syst. BP (mm Hg)	116±19	110±19	109±14	0.237	. . .	. . .	. . .
LVESVi (ml/m^2)	90±32	124±35	102±39	0.001	0.001	0.528	0.012
LVEDVi (ml/m^2)	117±36	147±39	125±41	0.007	0.010	0.993	0.032
LVEF (%)	22±6	16±4	20±7	0.001	0.001	0.931	0.003
LV sphericity	0.72±0.08	0.77±0.10	0.71±0.09	0.004	0.041	1.000	0.004
IVSd (mm)	9.1±1.3	8.4±1.6	8.8±2.0	0.317	. . .	. . .	. . .
LVPWd (mm)	9.3±1.7	9.7±1.7	8.8±1.8	0.063	. . .	. . .	. . .
S/P thickness ratio	1.0±0.2	0.9±0.2	1.0±0.2	0.004	0.090	1.000	0.003
MRero (mm^2)	6.1±5.9	10.2±7.4	9.9±8.0	0.061	. . .	. . .	. . .
Lead location (%)				0.689	. . .	. . .	. . .
(Postero)lateral	82	79	86				
Anterolateral	4	6	7				
Posterior	14	15	7				
Optimization (%)				0.470	. . .	. . .	. . .
Hemodynamic	79	65	69				
IEGM	21	35	31				

*Median and interquartile range. etiol. indicates etiology; segm., segments; Syst BP, systolic blood pressure; LVESVi, left ventricle (LV) end-systolic volume index: LVEDVi, LV end-diastolic volume index; LVEF, LV ejection fraction; LV sphericity, LV maximal short axis diameter divided by the maximal long axis diameter; IVSd, interventricular septum diastolic thickness; LVPWd, LV posterior wall diastolic thickness; S/P thickness ratio, IVSd/LVPWd; MRero, mitral regurgitation effective regurgitant orifice; IEGM, intracardiac electrogram algorithm.

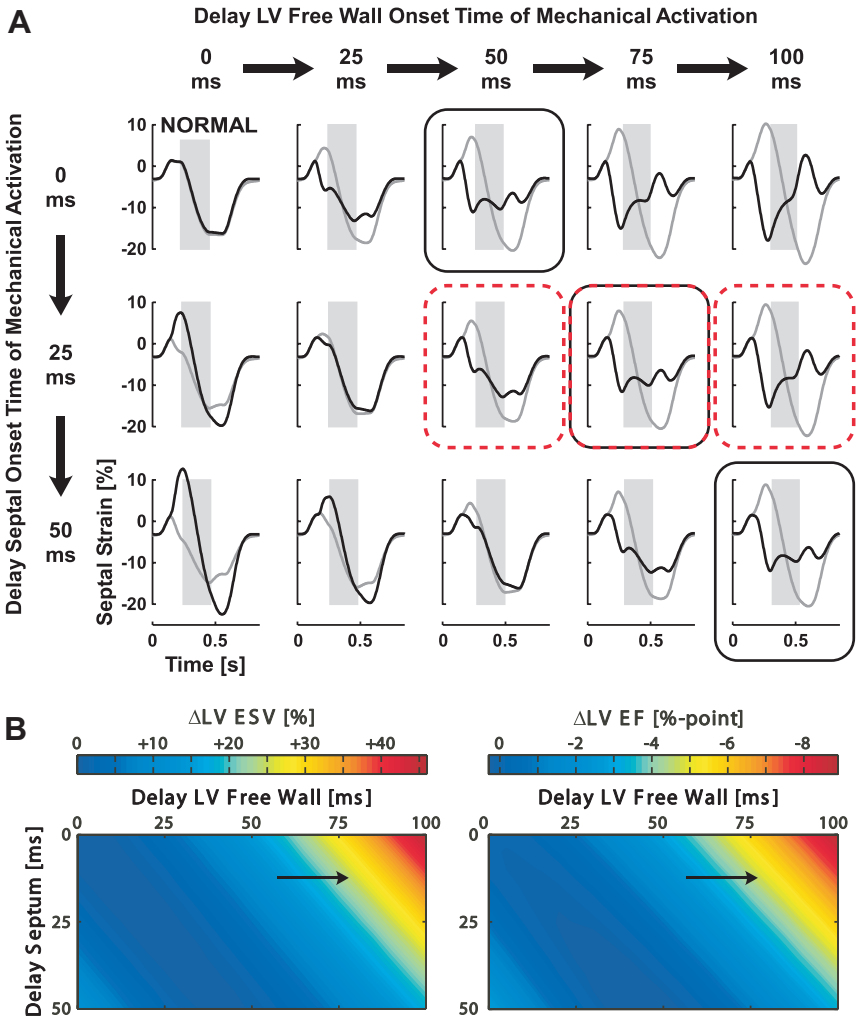

Figure 3. Effect of ventricular dyssynchrony on the septal deformation pattern and on global left ventricular (LV) pump function and dimension. **A**, Simulated septal myofiber strain (black lines) during a cardiac cycle with normal synchronous ventricular activation (NORMAL) and with dyssynchronous activation, that is, delayed onset of left ventricle free wall (left to right) and septal (top to bottom) activation with respect to right ventricle free wall activation. The left ventricle ejection period is highlighted in gray. Changes of intraventricular and interventricular mechanical delay are illustrated by red-dashed and solid black boxes, respectively. Left ventricle free wall strain is indicated by gray lines. **B**, Maps showing the relative change of left ventricle end-systolic volume (LVESV) and the absolute change of left ventricle ejection fraction (LVEF) because of dyssynchronous ventricular activation.

decreased LVEF, and decreased septal-to-posterior wall thickness ratio compared with the other 2 groups. LBBB-3 patients more often had ischemic heart failure etiology with a larger number of scarred segments throughout the LV, particularly in the LVFW, when compared with the other 2 groups, and had on average less electrical dyssynchrony.

Model Simulations

Effect of Ventricular Dyssynchrony on Septal Deformation

The septal deformation pattern in the NORMAL simulation showed continuous septal shortening during LV ejection. With progressive delay of LVFW activation (Figure 3A, upper row), an increasing part of septal shortening occurred before onset of LV ejection, in conjunction with an increase of septal rebound stretch during ejection. Conversely, progressively delaying septal activation (Figure 3A, left column) increased septal stretch before LV ejection. This prestretch in turn increased systolic septal shortening by a local Starling effect. The pattern of septal deformation appeared to be sensitive to changes of LV intraventricular (ie, septal to LVFW) delay rather than interventricular mechanical delay (ie, RV free wall to LVFW). For example, an intraventricular activation delay of 50 ms was consistently associated with a double-peaked septal deformation pattern. Similar to septal deformation pattern, LV end-systolic volume (LVESV) and LVEF strongly depended on intraventricular dyssynchrony (Figure 3B). With increasing septal to LVFW delay of activation, the LV dilated and its systolic pump function decreased. With 100 ms intraventricular delay, LVEF decreased by 9%-points, with LVESV increasing by 45%.

Effect of Regional Contractility Changes on Septal Deformation Pattern

Figure 4A shows the effect of regional LV myocardial contractility changes on the septal deformation pattern in case of 25 and 75 ms delay of septal and LV free wall activation, respectively. By decreasing septal contractility up to 60%, the septal deformation pattern gradually transformed into an early-peak pattern (Figure 4A, left column). On the other hand, a 60% decrease of LV free wall contractility lead to a late-peak pattern, irrespective of the presence of decreased septal contractility (Figure 4A, upper row and right column). Furthermore, the amount of septal systolic shortening decreased with decrease of septal contractility but increased with decrease of LV free wall contractility. Changes in systolic septal deformation were markedly less pronounced in the absence of dyssynchrony (online-only supplement). With

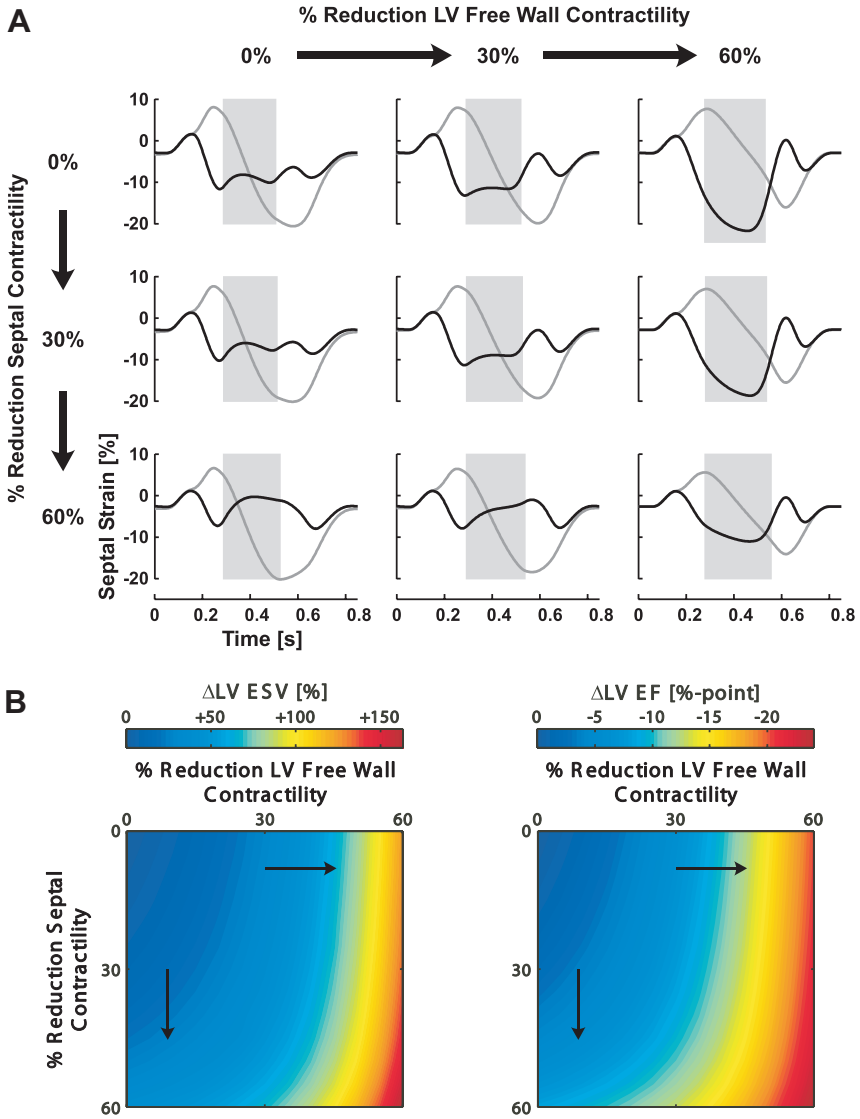

Figure 4. Effect of decreased myocardial contractility on the septal deformation pattern and on global left ventricular (LV) pump function and dimension. **A**, Simulated septal myofiber strain (black lines) in a heart with typical left bundle branch block dyssynchrony (25 and 75 ms delay of septal and left ventricle free wall activation, respectively), in combination with normal and regionally reduced left ventricle myocardial contractility. The left ventricle ejection period is highlighted in gray. Note that septal (from top to bottom) and left ventricle free wall (from left to right) hypocontractility affect the septal deformation pattern. Left ventricle free wall strain is indicated by gray lines. **B**, Maps showing the relative change of left ventricle end-systolic volume (LVESV) and the absolute change of left ventricle ejection fraction (LVEF) because of reduction of myocardial contractility.

decreasing septal or LV free wall contractility, LVEF decreased and LVESV progressively increased, both parameters being more sensitive to LVFW than to septal hypocontractility (Figure 4B).

Measured Versus Simulated Septal Deformation Patterns

The 3 characteristic septal deformation patterns, as measured in the patients, could also be identified in the simulations (Figure 5). The double-peaked LBBB-1 pattern was obtained by simulating typical LBBB dyssynchrony of ventricular activation. The early-peaked LBBB-2 pattern was obtained by additionally imposing septal hypocontractility. The late-peaked LBBB-3 pattern was obtained by simulation of dyssynchronous ventricular activation with decreased LVFW contractility, whether or not in combination with decreased septal contractility.

Response to CRT

After 6 months CRT, a significant reduction of LV volumes $LVESV_i$ 107±37 to 90±45 mL/m_2, $P<0.001$) and mitral regurgitation (MRero 9.2±7.4 to 6.0±6.1 mm^2, $P<0.001$), in combination with an improved LVEF (to 26±10%, $P<0.001$), was observed in the patients. There was a significant difference in response between the 3 subgroups (Table 2). Reverse remodeling and improvement of LVEF were most pronounced in patients with LBBB-1. Patients with LBBB-2 also showed significant, but less, remodeling and improvement of systolic function. Patients with LBBB-3 did not show a significant echocardiographic response to CRT, which was also significantly less compared with the other 2 groups.

Discussion

In this study, we demonstrated within a typical CRT patient population the presence of 3 characteristic septal deformation patterns that showed a different response to CRT. Using the CircAdapt model, we were able to demonstrate that these patterns can be explained by various combinations of intraventricular dyssynchrony and regional contractility. Therefore, septal deformation provides integrated information on 2 key determinants of CRT response: dyssynchrony and reduced regional LV myocardial contractility.

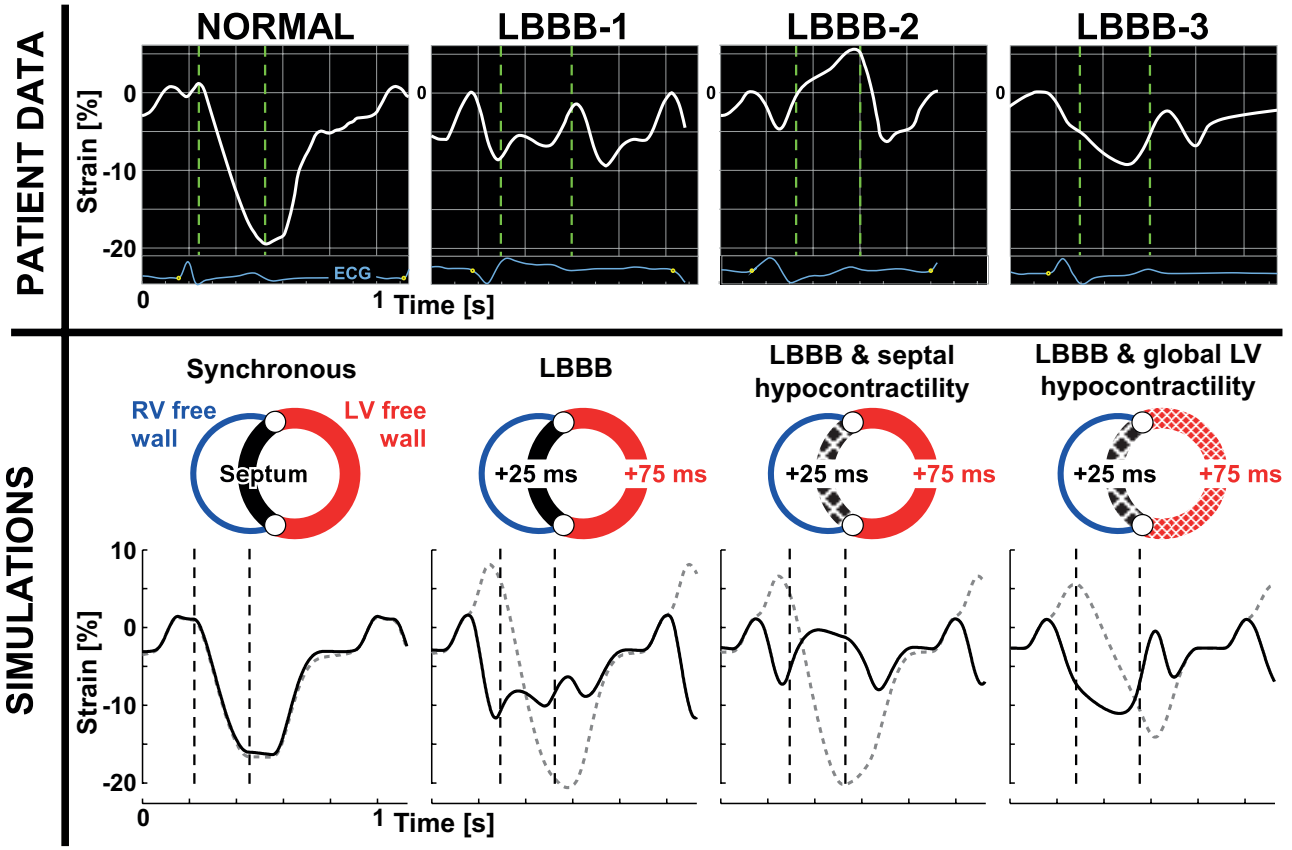

Figure 5. Comparison of measured and simulated septal deformation patterns. For a normal healthy subject (NORMAL) and 3 typical patients each representing 1 of the left bundle branch block (LBBB) subgroups (LBBB-1, LBBB-2, and LBBB-3), septal deformation patterns in the upper panels are compared with the model simulations in the lower panels (septal and left ventricle [LV] free wall strain indicated by solid and dashed lines, respectively). Vertical dashed lines indicate aortic valve opening and closure. Starting from the normal simulation (lower left corner), similar characteristic septal deformation patterns are obtained as measured in the study population by simple model simulations, that is, classical LBBB (25 and 75 ms delay of septal and left ventricle free wall activation, respectively) with normal myocardial contractility (LBBB-1), LBBB with additional septal hypocontractility (LBBB-2), and LBBB with additional septal and left ventricle free wall hypocontractility (LBBB-3).

Impact of Dyssynchrony on Septal Deformation

The findings in both the model and the patients indicate that the double-peaked LBBB-1 pattern is the uncomplicated septal deformation pattern in the presence of LBBB. The premature interruption of early systolic shortening with systolic rebound stretch that determines the first part of this pattern is a characteristic feature of regional electrical preexcitation and has been described in ventricular pacing,[28–30] accessory atrioventricular pathways,[31,32] and LBBB.[3,5,6,32] In the case of LBBB, the early vigorous septal shortening has been ascribed to low local afterload during early activation. The model also indicates that the remaining part of the complicated septal deformation pattern in LBBB can be attributed to dyssynchronous activation, without additional alterations in myocardial tissue properties or loading conditions. The subsequent local rebound stretch in the septum most probably results from an imbalance in tensional forces between the early activated septum and the later activated LVFW, whereas the second shortening peak, observed in LBBB-1, indicates re-equilibration of these forces later in systole.

The simulations also indicate that LV intraventricular, rather than interventricular dyssynchrony, is the main deter-

Table 2. Echocardiographic Response of Septal Deformation Pattern Subgroups

	Septal Deformation Pattern			*P* Value			
Parameter	LBBB-1	LBBB-2	LBBB-3	ANOVA/χ^2	LBBB-1 vs LBBB-2	LBBB-1 vs LBBB-3	LBBB-2 vs LBBB-3
ΔLVEDVi (%)	26±17	16±22	2±16	<0.001	0.137	<0.001	0.002
ΔLVESVi (%)	37±20	24±24	5±20	<0.001	0.068	<0.001	0.001
ΔLVEF (%-point)	13±9	8±7	3±7	<0.001	0.021	<0.001	0.007
ΔMRero (%)	58±42	20±59	21±49	0.012	0.028	0.015	1.000

LVEDVi indicates LV end-diastolic volume index; $LVESV_i$, LV end-systolic volume index; LVEF, LV ejection fraction; MRero, mitral regurgitation effective regurgitant orifice.

minant of septal deformation. This finding may seem in contrast with previous echocardiographic M-mode studies attributing the observed motion abnormalities mainly to abnormal interventricular coupling and the resulting transseptal pressure gradient.[4,33] Interventricular interaction and intraventricular dyssynchrony do, however, closely intertwine, and intraventricular dyssynchrony almost inevitably leads to an abnormal transseptal pressure gradient.[4,5,9] Our findings do not preclude an effect of interventricular coupling on septal deformation. They rather indicate that the interactions are initiated by LV intraventricular dyssynchrony and that the timing of activation of the RV free wall is of minor importance.

Modification of Septal Deformation by Regional Contractility Changes

The model study furthermore indicates that, on top of dyssynchrony, regional contractility influences septal deformation. Pattern LBBB-2 and LBBB-3 were derived from the LBBB-1 pattern by reduction of septal and LVFW contractility, respectively. It thus appears that reduction of septal contractility precludes the equilibration of contractile forces during late systole, while the relatively unopposed early shortening remains unaffected. On the other hand, reduction of LVFW contractility reduces the stretching forces imposed on the septum, thus allowing the septal contraction to be extended further into systole. The fact that contractility changes alone could not induce an early systolic shortening peak further confirms the specificity of this pattern as a marker of electrical dyssynchrony (online-only supplement).

The computer simulation does not distinguish between various causes of hypocontractility. In patients, the cause could be either scar of an old infarct, hibernation, or localized disease-specific processes. In the patients, we found an increased amount of (LVFW) scar in conjunction with the LBBB-3 pattern, fitting with the reduced LVFW contractility required to obtain this pattern in the model (Table 1). In LBBB-2 patients, however, we did not find an increased amount of septal scar, whereas the LBBB-2 simulation required the reduction of septal contractility. Alternatively, hibernation, echocardiographically undetectable midseptal scarring,[34] or advanced LBBB-specific remodeling processes[3,29,35] might explain the relatively reduced septal contractility, the latter being partly supported by the more pronounced remodeling in those patients (Table 1).

Relation of Septal Deformation With CRT Response

In previous studies, it has been demonstrated that the extent of dyssynchrony-induced deformation abnormalities (expressed as systolic rebound stretch in the entire LV or in the septum alone) relates to the functional impact of dyssynchrony and the benefit of resynchronization.[6] This observation is in agreement with the demonstration in this study that septal deformation is directly linked to dyssynchronous activation within the LV, a recognized electro-mechanical substrate for CRT. In our simulations, application of dyssynchrony induced changes in global LV function and dimensions comparable to those observed in canine LBBB hearts.[3,36] It is worth noting that in the model, cardiac output and mean arterial blood pressure were kept constant. In vivo, pump function is reduced immediately after inducing dyssynchrony, but (partly) recovers after some time, because of autonomic and renal compensation mechanisms. Therefore, the extent of increase in LVESV, and decrease in LVEF in the model, are more in line with changes after longer lasting LBBB than acutely after LBBB.

Previous studies have indicated that LV scarring reduces CRT response, especially when located in the posterolateral region.[12,13] This has been attributed mainly to pacing delivery failure and lack of recruitable myocardium. Additionally, the results in the current study indicate that extensive LV hypocontractility might mitigate the translation of electrical dyssynchrony into mechanical discoordination. Accordingly, the presence of LVFW hypocontractility resulted in less discoordinate septal deformation with little systolic rebound stretch (ie, LBBB-3), and likewise, with a smaller benefit of CRT. The moderate response in the LBBB-2 patients, on the other hand, can be explained by the reduced amount of septal contractility that can be recruited by CRT, either because of scarring or because of extensive and partly irreversible remodeling.[37]

Potential Clinical Implications

The finding that uncomplicated LBBB results in double-peaked septal deformation demonstrates that assessment of dyssynchrony by time-to-peak measurements is not straightforward.[6,38] Our data further demonstrate that, at the same intraventricular dyssynchrony, the peak shortening time depends on contractility of the septum and LVFW. These factors may explain why several studies showed a poor relation between time-to-peak measurements and CRT response. Conversely, our data suggest that the septal deformation pattern provides integrated information on intraventricular dyssynchrony and regional LV scarring, 2 important determinants of CRT response. Assessment of septal deformation, potentially assisted by a patient computer model, might, therefore, provide an alternative to multimodality assessment (ie, echocardiography and magnetic resonance imaging or myocardial scintigraphy) before CRT.

Limitations

In our model, each of the 3 ventricular walls was lumped into a spherical wall segment containing a single contractile fiber describing representative passive and active sarcomere properties of the entire wall.[2] This simplified setup allows inhomogeneity of material properties between ventricular walls but does not allow local inhomogeneities within a wall. Despite the inherent limitations, this provides a clearer mechanistic view, because of less alternating parameters. The qualitative and sometimes quantitative agreement between the model simulations and the clinical measurements of septal deformation indicate that the simplifications made in the simulations do not obscure first-order effects of ventricular mechanical dyssynchrony and hypocontractility on the septal deformation pattern.

We used the echocardiographic aspect of the myocardium to diagnose the presence of scar. Although this is an accepted

approach,[17] the use of late gadolinium-enhanced magnetic resonance imaging might have revealed additional areas of (more subtle) scarring.

Because the current study is the first study investigating the interrelation between dyssynchrony, contractility, and septal deformation, its design was mainly exploratory without predefined specific cut-offs for a clinically relevant magnitude of the differences. Also, only patient data from a single institution were analyzed. The results, therefore, need to be confirmed in a prospective multicenter study. In addition, future studies should establish whether the current findings can be generalized to patients with less severe heart failure.

Conclusion

The pattern of septal deformation is highly sensitive to ventricular dyssynchrony and regional differences in myocardial contractility and thereby predicts CRT response. Model simulations can extract otherwise concealed diagnostic information from the septal deformation patterns as measured in the patients.

Disclosures

This research was performed within the framework of CTMM, the Center for Translational Molecular Medicine (www.ctmm.nl), project COHFAR (grant 01C-203), and is supported by the Dutch Heart Foundation. Dr Prinzen has also received research grants from EBR Systems and Merck Sharp & Dohme.

References

1. Auricchio A, Fantoni C, Regoli F, Carbucicchio C, Goette A, Geller C, Kloss M, Klein H. Characterization of left ventricular activation in patients with heart failure and left bundle-branch block. *Circulation*. 2004;109:1133–1139.
2. Rodriguez LM, Timmermans C, Nabar A, Beatty G, Wellens HJ. Variable patterns of septal activation in patients with left bundle branch block and heart failure. *J Cardiovasc Electrophysiol*. 2003;14:135–141.
3. Vernooy K, Verbeek XA, Peschar M, Crijns HJ, Arts T, Cornelussen RN, Prinzen FW. Left bundle branch block induces ventricular remodelling and functional septal hypoperfusion. *Eur Heart J*. 2005;26:91–98.
4. Little WC, Reeves RC, Arciniegas J, Katholi RE, Rogers EW. Mechanism of abnormal interventricular septal motion during delayed left ventricular activation. *Circulation*. 1982;65:1486–1491.
5. Gjesdal O, Remme EW, Opdahl A, Skulstad H, Russell K, Kongsgaard E, Edvardsen T, Smiseth OA. Mechanisms of abnormal systolic motion of the interventricular septum during left bundle-branch block. *Circ Cardiovasc Imaging*. 2011;4:264–273.
6. De Boeck BW, Teske AJ, Meine M, Leenders GE, Cramer MJ, Prinzen FW, Doevendans PA. Septal rebound stretch reflects the functional substrate to cardiac resynchronization therapy and predicts volumetric and neurohormonal response. *Eur J Heart Fail*. 2009;11:863–871.
7. Jansen AH, van Dantzig JM, Bracke F, Meijer A, Peels KH, van den Brink RB, Cheriex EC, Delemarre BJ, van der Wouw PA, Korsten HH, van Hemel NM. Qualitative observation of left ventricular multiphasic septal motion and septal-to-lateral apical shuffle predicts left ventricular reverse remodeling after cardiac resynchronization therapy. *Am J Cardiol*. 2007;99:966–969.
8. Parsai C, Bijnens B, Sutherland GR, Baltabaeva A, Claus P, Marciniak M, Paul V, Scheffer M, Donal E, Derumeaux G, Anderson L. Toward understanding response to cardiac resynchronization therapy: left ventricular dyssynchrony is only one of multiple mechanisms. *Eur Heart J*. 2009;30:940–949.
9. Leenders GE, Cramer MJ, Bogaard MD, Meine M, Doevendans PA, De Boeck BW. Echocardiographic prediction of outcome after cardiac resynchronization therapy: conventional methods and recent developments. *Heart Fail Rev*. 2011;16:235–250.
10. Dillon JC, Chang S, Feigenbaum H. Echocardiographic manifestations of left bundle branch block. *Circulation*. 1974;49:876–880.
11. Skulstad H, Urheim S, Edvardsen T, Andersen K, Lyseggen E, Vartdal T, Ihlen H, Smiseth OA. Grading of myocardial dysfunction by tissue Doppler echocardiography: a comparison between velocity, displacement, and strain imaging in acute ischemia. *J Am Coll Cardiol*. 2006;47:1672–1682.
12. Bleeker GB, Kaandorp TA, Lamb HJ, Boersma E, Steendijk P, de RA, van der Wall EE, Schalij MJ, Bax JJ. Effect of posterolateral scar tissue on clinical and echocardiographic improvement after cardiac resynchronization therapy. *Circulation*. 2006;113:969–976.
13. Ypenburg C, Schalij MJ, Bleeker GB, Steendijk P, Boersma E, Dibbets–Schneider P, Stokkel MP, van der Wall EE, Bax JJ. Impact of viability and scar tissue on response to cardiac resynchronization therapy in ischaemic heart failure patients. *Eur Heart J*. 2007;28:33–41.
14. Arts T, Delhaas T, Bovendeerd P, Verbeek X, Prinzen FW. Adaptation to mechanical load determines shape and properties of heart and circulation: the CircAdapt model. *Am J Physiol Heart Circ Physiol*. 2005;288:H1943–H1954.
15. Lumens J, Delhaas T, Kirn B, Arts T. Three-wall segment (TriSeg) model describing mechanics and hemodynamics of ventricular interaction. *Ann Biomed Eng*. 2009;37:2234–2255.
16. Schiller NB, Shah PM, Crawford M, DeMaria A, Devereux R, Feigenbaum H, Gutgesell H, Reichek N, Sahn D, Schnittger I. Recommendations for quantitation of the left ventricle by two-dimensional echocardiography. American Society of Echocardiography Committee on Standards, Subcommittee on Quantitation of Two-Dimensional Echocardiograms. *J Am Soc Echocardiogr*. 1989;2:358–367.
17. Faletra F, Crivellaro W, Pirelli S, Parodi O, De CF, Cipriani M, Corno R, Pezzano A. Value of transthoracic two-dimensional echocardiography in predicting viability in patients with healed Q-wave anterior wall myocardial infarction. *Am J Cardiol*. 1995;76:1002–1006.
18. Lumens J, Arts T, Broers B, Boomars KA, van PP, Prinzen FW, Delhaas T. Right ventricular free wall pacing improves cardiac pump function in severe pulmonary arterial hypertension: a computer simulation analysis. *Am J Physiol Heart Circ Physiol*. 2009;297:H2196–H2205.
19. Kerckhoffs RC, Lumens J, Vernooy K, Omens JH, Mulligan LJ, Delhaas T, Arts T, McCulloch AD, Prinzen FW. Cardiac resynchronization: insight from experimental and computational models. *Prog Biophys Mol Biol*. 2008;97:543–561.
20. Lumens J, Delhaas T, Kirn B, Arts T. Modeling ventricular interaction: a multiscale approach from sarcomere mechanics to cardiovascular system hemodynamics. *Pac Symp Biocomput*. 2008;378–389.
21. de Tombe PP, ter Keurs HE. Force and velocity of sarcomere shortening in trabeculae from rat heart. Effects of temperature. *Circ Res*. 1990;66:1239–1254.
22. de Tombe PP. Cardiac myofilaments: mechanics and regulation. *J Biomech*. 2003;36:721–730.
23. ter Keurs HE, Rijnsburger WH, van HR, Nagelsmit MJ. Tension development and sarcomere length in rat cardiac trabeculae. Evidence of length-dependent activation. *Circ Res*. 1980;46:703–714.
24. Baker AE, Dani R, Smith ER, Tyberg JV, Belenkie I. Quantitative assessment of independent contributions of pericardium and septum to direct ventricular interaction. *Am J Physiol*. 1998;275:H476–H483.
25. Belenkie I, Dani R, Smith ER, Tyberg JV. The importance of pericardial constraint in experimental pulmonary embolism and volume loading. *Am Heart J*. 1992;123:733–742.
26. Belenkie I, Sas R, Mitchell J, Smith ER, Tyberg JV. Opening the pericardium during pulmonary artery constriction improves cardiac function. *J Appl Physiol*. 2004;96:917–922.
27. Morris-Thurgood JA, Frenneaux MP. Diastolic ventricular interaction and ventricular diastolic filling. *Heart Fail Rev*. 2000;5:307–323.
28. Prinzen FW, Hunter WC, Wyman BT, McVeigh ER. Mapping of regional myocardial strain and work during ventricular pacing: experimental study using magnetic resonance imaging tagging. *J Am Coll Cardiol*. 1999;33:1735–1742.
29. Prinzen FW, Augustijn CH, Arts T, Allessie MA, Reneman RS. Redistribution of myocardial fiber strain and blood flow by asynchronous activation. *Am J Physiol*. 1990;259:H300–H308.
30. Wyman BT, Hunter WC, Prinzen FW, McVeigh ER. Mapping propagation of mechanical activation in the paced heart with MRI tagging. *Am J Physiol*. 1999;276:H881–H891.
31. De Boeck BW, Teske AJ, Leenders GE, Mohamed Hoesein FA, Loh P, van DV, Doevendans PA, Prinzen FW, Cramer MJ. Detection and quantification by deformation imaging of the functional impact of septal compared to free wall preexcitation in the Wolff-Parkinson-White syndrome. *Am J Cardiol*. 2010;106:539–546.

32. De Boeck BW, Kirn B, Teske AJ, Hummeling RW, Doevendans PA, Cramer MJ, Prinzen FW. Three-dimensional mapping of mechanical activation patterns, contractile dyssynchrony and dyscoordination by two-dimensional strain echocardiography: rationale and design of a novel software toolbox. *Cardiovasc Ultrasound*. 2008;6:22.
33. Grines CL, Bashore TM, Boudoulas H, Olson S, Shafer P, Wooley CF. Functional abnormalities in isolated left bundle branch block. The effect of interventricular asynchrony. *Circulation*. 1989;79:845–853.
34. Wu KC, Weiss RG, Thiemann DR, Kitagawa K, Schmidt A, Dalal D, Lai S, Bluemke DA, Gerstenblith G, Marban E, Tomaselli GF, Lima JA. Late gadolinium enhancement by cardiovascular magnetic resonance heralds an adverse prognosis in nonischemic cardiomyopathy. *J Am Coll Cardiol*. 2008;51:2414–2421.
35. Prinzen FW, Cheriex EC, Delhaas T, van Oosterhout MF, Arts T, Wellens HJ, Reneman RS. Asymmetric thickness of the left ventricular wall resulting from asynchronous electric activation: a study in dogs with ventricular pacing and in patients with left bundle branch block. *Am Heart J*. 1995;130:1045–1053.
36. Verbeek XA, Vernooy K, Peschar M, Cornelussen RN, Prinzen FW. Intra-ventricular resynchronization for optimal left ventricular function during pacing in experimental left bundle branch block. *J Am Coll Cardiol*. 2003;42:558–567.
37. Bax JJ, Schinkel AF, Boersma E, Elhendy A, Rizzello V, Maat A, Roelandt JR, van der Wall EE, Poldermans D. Extensive left ventricular remodeling does not allow viable myocardium to improve in left ventricular ejection fraction after revascularization and is associated with worse long-term prognosis. *Circulation.* 2004;110:II18–II22.
38. Russell K, Opdahl A, Remme EW, Gjesdal O, Skulstad H, Kongsgaard E, Edvardsen T, Smiseth OA. Evaluation of left ventricular dyssynchrony by onset of active myocardial force generation: a novel method that differentiates between electrical and mechanical etiologies. *Circ Cardiovasc Imaging*. 2010;3:405–414.

CLINICAL PERSPECTIVE

Dyssynchrony and regional contractility reduction (eg, by left ventricular scarring or localized remodeling processes) are 2 key determinants of cardiac resynchronization therapy response. The current study assessed the influence of both factors on the deformation pattern of the interventricular septum in patients and in a computer model of the heart and circulation. By using this combined approach, we demonstrate that combinations of dyssynchrony and reduced regional contractility result in 3 characteristic septal deformation patterns, each associated with a different clinical response chance. “Isolated” left bundle branch block (LBBB), that is, substantially delayed activation of the left ventricle free wall with normal contractility, resulted in double-peaked systolic shortening (LBBB-1). LBBB with septal hypocontractility resulted in an early-systolic shortening peak followed by prominent systolic stretching (LBBB-2), whereas LBBB with left ventricle free wall or global hypocontractility resulted in pseudonormal systolic shortening with a late-systolic peak (LBBB-3). Improvement of left ventricle ejection fraction and reduction of left ventricle volumes after cardiac resynchronization therapy were most pronounced in LBBB-1 and worst in LBBB-3 patients. The current study indicates that the pattern of septal deformation can be used to infer information on the presence of substantial dyssynchrony and reduced regional contractility. The study also indicates that assessment of septal deformation patterns, assisted by a personalized computer model, may further improve the prediction of cardiac resynchronization therapy response. Finally, double-peaked patterns, and the sensitivity of the patterns to regional contractility, illustrate the practical and conceptual limitations of time-to-peak measurements (dyssynchrony) to predict cardiac resynchronization therapy response.

SUPPLEMENTAL MATERIAL

Supplemental methods

Pericardium

In several studies, it has been shown that the pericardium significantly modulates ventricular interaction.[1-4] Since ventricular interaction has been suggested to play an important role during left ventricular (LV) pacing,[5, 6] we included the pericardium in the CircAdapt model. The passive mechanical behavior of the pericardium was modeled by a pericardial pressure acting on the epicardium of the LV and RV free walls as well as of the atria (Figure S1). Consequently, transmural pressure across the LV free wall equals LV cavity pressure minus pericardial pressure whereas transmural pressure across the RV free wall equals RV cavity pressure minus pericardial pressure. Similarly, transmural pressure across the atrial walls equals atrial cavity pressure minus pericardial pressure. Moreover, the external pressure surrounding the pericardium is assumed to be zero. Instantaneous pericardial pressure p_{peri} depends on pericardial volume V_{peri} by

$$p_{peri}(t) = p_{ref} \cdot \left(\frac{V_{peri}(t)}{V_{ref}} \right)^{10}$$

where the constants p_{ref} and V_{ref} represent reference pericardial pressure and volume, respectively. In experimental animals[7] as well as in patients,[8] the pericardium has been shown to be capable of adapting over time to changes in cardiac size. In our NORMAL model simulation, the pericardium is assumed to be adapted to a moderate level of exercise (3x resting cardiac output and 2x resting heart rate), i.e., V_{ref} is adapted so that mean pericardial pressure amounts to the preset value p_{ref} of 4 mmHg. In all other

simulations, the pericardium was not further adapted, i.e., passive pericardial material properties were identical in all simulations.

Supplemental results

Effect of regional LV contractility changes on septal deformation pattern in the absence of ventricular dyssychrony

Figure S2A shows the isolated effect of regional LV myocardial contractility changes on the septal deformation pattern in a heart with normal (synchronous) activation of the ventricular walls. As in the dyssynchronous simulations, the amount of septal systolic shortening decreased with decrease of septal contractility, whereas it increased with decrease of LV free wall contractility. The majority of the dyssynchronous simulations however, were characterized by an early systolic peak. This peak only disappeared in case of severely decreased LV free wall contractility, transforming the septal deformation pattern into a pattern with a late systolic peak (Figure 4A). Conversely, isolated regional decrease of contractility in the absence of dyssynchrony did not result in an early systolic shortening peak. Decrease of septal contractility rather resulted in pronounced septal stretch before ejection and an extremely late postsystolic septal shortening peak. Decrease of LV free wall contractility on the other hand, resulted in a similar late-systolic peak as observed in dyssynchronous hearts with reduced LV free wall contractility (Figure S2A), but with less pronounced systolic rebound stretch after the peak. Figure S2B shows the changes of LV systolic pump function as a result of septal and LV free wall hypocontractility in the normal heart. Similar to the dyssynchronous simulations, decreases of septal or LV free wall contractility lead to a deterioration of global LV pump

function as evidenced by the increase of LV end-systolic volume and the decrease of LV ejection fraction.

Supplemental figures and figure legends

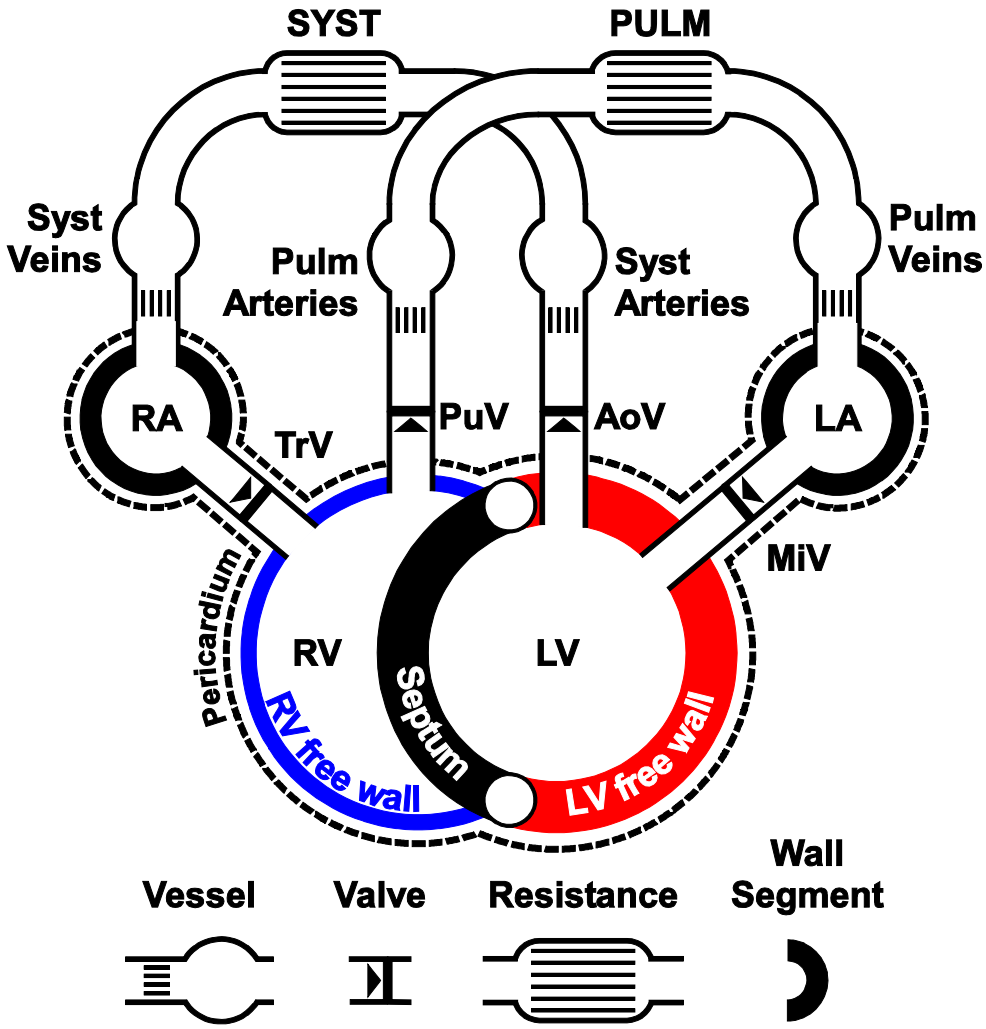

Figure S1: Schematic representation of the CircAdapt model

The CircAdapt model is designed as a network of modules representing myocardial walls, valves, large blood vessels, and peripheral resistances. The ventricular cavities are surrounded by three thick-walled segments representing the left ventricular (LV) free

wall, the right ventricular (RV) free wall, and the septum. The pericardium is modeled as a passive sheet surrounding the ventricles and atria. The pulmonary (Pulm) and systemic (Syst) circulations enable hemodynamic interaction between the left and right side of the heart. Abbreviations: AoV = aortic valve; LA = left atrium; MiV = mitral valve; PuV = pulmonary valve; RA = right atrium; and TrV = tricuspid valve.

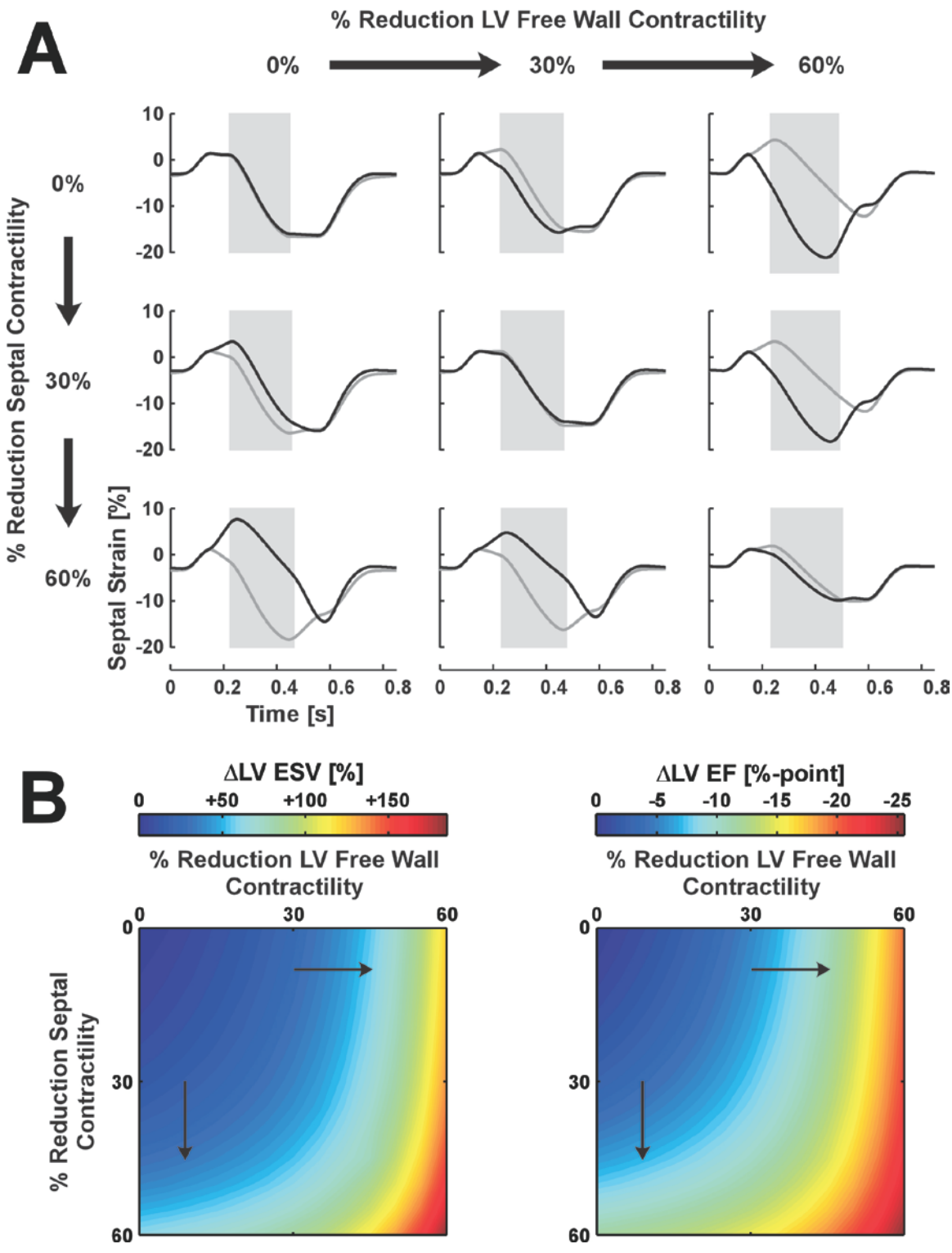

Figure S2: Effect of decreased myocardial contractility on the septal deformation pattern and on global left ventricular pump function and dimension in the absence of ventricular dyssynchrony.

A: Simulated septal myofiber strain (black lines) in a heart with normal synchronous ventricular activation in combination with normal and regionally reduced LV myocardial contractility. The LV ejection period is highlighted in grey. LVFW strain is indicated by grey lines. Note that, according to the model, an early systolic peak does not occur as a result of isolated contractility differences in the absence of dyssynchrony. **B:** Maps showing the relative change of LV end-systolic volume (ESV) and the absolute change of LV ejection fraction (EF) due to reduction of myocardial contractility.

Supplemental References

(1) Baker AE, Dani R, Smith ER, Tyberg JV, Belenkie I. Quantitative assessment of independent contributions of pericardium and septum to direct ventricular interaction. *Am J Physiol* 1998;275:H476-H483.

(2) Belenkie I, Dani R, Smith ER, Tyberg JV. The importance of pericardial constraint in experimental pulmonary embolism and volume loading. *Am Heart J* 1992;123:733-42.

(3) Belenkie I, Sas R, Mitchell J, Smith ER, Tyberg JV. Opening the pericardium during pulmonary artery constriction improves cardiac function. *J Appl Physiol* 2004;96:917-22.

(4) Morris-Thurgood JA, Frenneaux MP. Diastolic ventricular interaction and ventricular diastolic filling. *Heart Fail Rev* 2000;5:307-23.

(5) Bleasdale RA, Turner MS, Mumford CE, Steendijk P, Paul V, Tyberg JV, Morris-Thurgood JA, Frenneaux MP. Left ventricular pacing minimizes diastolic ventricular interaction, allowing improved preload-dependent systolic performance. *Circulation* 2004;110:2395-400.

(6) Morris-Thurgood JA, Turner MS, Nightingale AK, Masani N, Mumford C, Frenneaux MP. Pacing in heart failure: improved ventricular interaction in diastole rather than systolic re-synchronization. *Europace* 2000;2:271-5.

(7) Freeman GL, LeWinter MM. Pericardial adaptations during chronic cardiac dilation in dogs. *Circ Res* 1984;54:294-300.

(8) Blanchard DG, Dittrich HC. Pericardial adaptation in severe chronic pulmonary hypertension. An intraoperative transesophageal echocardiographic study. *Circulation* 1992;85:1414-22.